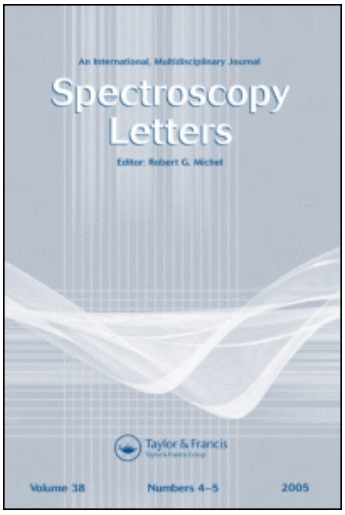

Spectroscopy Letters
Publication details, including instructions for authors and subscription information:
http://www.informaworld.com/smpp/title~content=t713597299

^{1}H NMR AND OPTICAL SPECTROSCOPY STUDY OF THE RADIODOSIMETRIC PROPERTIES OF THE PIRA GEL

G. Zebrowska[a]; Cz. Lewa[b]; J. de Certaines[b]
[a] Université de Rennes I, Rennes, Cedex, France [b] Institute of Experimental Physics, University of Gdansk, Gdansk, Poland

Online publication date: 31 October 2001

To cite this Article Zebrowska, G. , Lewa, Cz. and de Certaines, J.(2001) ''H NMR AND OPTICAL SPECTROSCOPY STUDY OF THE RADIODOSIMETRIC PROPERTIES OF THE PIRA GEL', Spectroscopy Letters, 34: 5, 549 — 567
To link to this Article: DOI: 10.1081/SL-100106870
URL: http://dx.doi.org/10.1081/SL-100106870

SPECTROSCOPY LETTERS, 34(5), 549–567 (2001)

^{1}H NMR AND OPTICAL SPECTROSCOPY STUDY OF THE RADIODOSIMETRIC PROPERTIES OF THE PIRA GEL

G. Zebrowska,[1,2] Cz. Lewa,[2] and J. de Certaines[2,3]

[1]Laboratoire de Résonance Magnétique en Biologie et Médecine, Université de Rennes I, 35043 Rennes Cedex, France
[2]Institute of Experimental Physics, University of Gdansk, ul. Wita Stwosza 57, 80-952 Gdansk, Poland
[3]Centre Eugène Marquis, 35062 Rennes Cedex, France

ABSTRACT

The radiation-response of the Fricke-doped protein-polymer gel (PIRA) was studied by ^{1}H NMR, as well as with spectrophotometric and fluorescence methods. In this gel, the ionizing radiation induces an increase in the NMR longitudinal relaxation rate, $R1$, of protons. It was observed that: I) the main mechanism responsible for the increase in $R1$ was the oxidation of ferrous to ferric ions; ii) the total amount of acrylamide with the same weight fraction (50%C) of the cross-linker N,N′-methylene-bis-acrylamide in the range 6%—12% by weight had no effect upon the $R1$ dose sensitivity; iii) the increase in the bovine serum albumin (BSA) concentration caused a drop in the $R1$ dose response sensitivity; iv) the $R1$ dose sensitivity was pH dependent. The four-site fast exchange model for $R1$ dose response was applied to calculate the ferric ions chemical yield $G(Fe^{3+})$. The $G(Fe^{3+})$ value obtained from

the NMR data agreed with that determined independently from spectrophotometric measurements.

Key Words: MRI dosimetry; Proton relaxation times; Fluorescence; Protein-polymer gel (PIRA); Phantom material; Fricke-doped gels

INTRODUCTION

In 1984, Gore *et al*. first demonstrated the possibility of detecting the spatial distribution of an absorbed dose in phantom material by the use of Magnetic Resonance Imaging (MRI), based on the dosimetric properties of the Fricke solution[1,2]. Since then, several NMR dosimeter substances have been proposed for dose distribution imaging. Their characteristic features are: i) a dosimeter component changing in accordance with the absorbed dose and influencing the proton relaxation times, e.g. the concentration of ferric ions formed as a result of the oxidation of ferrous ions[3,4], or the formation of crosslinked polymers[5,6]; ii) a gel matrix substance[7–12]; iii) similarity to real tissue[13,14]; and iv) sensitivity to ionizing radiation[15–17]. Compared with other dosimetry methods, NMR dosimetry could be particularly useful for verification of complex irradiation geometries using multibeam techniques and including mixed modalities, if their uncertainty fulfills the dose criteria required for radiotherapy measurements[18–22]. This goal can be achieved by standardization of the gel preparing protocol[23,24], improving the resolution and accuracy of the measurement methods[25–27], and finally, by thorough determination of the ionizing radiation induced mechanisms that influence proton relaxation times[28–30]. Recently, Audet and Schreiner[30] presented a multiple-site fast exchange model for spin-lattice relaxation in the Fricke gelatin dosimeter gel. This model is an extension of the model developed previously for aqueous Fricke dosimeters[31] and concerns two mechanisms governing the dose response of the ferrous sulphate-doped dosimeter gels. The first mechanism is the chemical response of the dosimetric component, the second one covers the effect of the ferric ions produced in the gel by radiation-induced oxidation of the ferrous ions upon NMR spin-lattice relaxation.

The aim of this paper was to apply this model to the PIRA gel, as proposed by Zebrowska *et al*.[12], and to verify its usefulness for absolute dosimetry. The PIRA gel is a test substance, including the same dosimeter component (the Fricke solution), but with a significantly different gel matrix, associating bovine serum albumin (BSA) with acrylamide and N,N′-methylene-bis-acrylamide (often used in electrophoresis techniques).

MARCEL DEKKER, INC.
270 Madison Avenue, New York, New York 10016

Apart from the usefulness of the PIRA gel in the spatial determination of the absorbed dose of ionizing radiation by MRI, it shows closer similarity to soft biological tissues in the elemental composition, mass density and electron density, compared to the previously described Fricke-doped dosimetric gels[32].

Spectrophotometric and fluorescence spectroscopy measurements were also performed to elucidate the radio-induced mechanisms which could be responsible for the increase in the proton longitudinal relaxation rate ($R1$) with the absorbed dose. From the absorbance data one can obtain information on Fe^{3+} ion concentration and, consequently, determine the gel radiosensitivity, as well as calculate the ferric ion G value (number of Fe^{3+} ions produced per 100 eV) independent of its determination by the NMR study. Other properties of the gel that can influence its radiosensitivity and the measured R1 can be obtained from fluorescence measurements of the luminescent probes doped to the sample[33]. For example, alterations in the emission spectra of some luminescent probes afford information on structural changes in the medium. Emission anisotropy values are sensitive to the probe rigidity, indicating modifications in the gel matrix condition.

MATERIALS AND METHODS

Sample Preparation

The PIRA tissue equivalent gel consists of 5% by weight bovine serum albumin (BSA) (A-7030, Sigma Chimie, St. Quentin Fallavier, France), 10% by weight acrylamide (A-3553, Sigma Chimie, St. Quentin Fallavier, France) with 50%C N,N′-methylene-bis- acrylamide (bis) (A-M-7279, Sigma Chimie, St. Quentin Fallavier, France), 0.5 mM $Fe(NH_4)_2(SO_4)_2 \times 6H_2O$ (F-3754, Sigma Chimie, St. Quentin Fallavier, France), 100 mM H_2SO_4 (analytical grade) and high-purity water. Detailed procedures for the preparation of the PIRA gel were reported elsewhere[32]. To determine the optimum proportion of the gel compounds and the mechanisms governing dose response, different concentrations were examined (Table 1).

All the Fe^{2+} and Fe^{3+} solutions were prepared by dissolving $Fe(NH_4)_2(SO_4)_2 \times 6H_2O$ and $FeNH_4(SO_4)_2 \times 12H_2O$ (F-3629, Sigma Chemical, Germany) in high-purity water and H_2SO_4 (analytical grade), respectively.

The PIRA gel samples for fluorescence measurements were prepared with pyrene as a flourescent probe. Pyrene was added to BSA solution during the gel preparation. The final concentration of pyrene was fixed at 1×10^{-5} M.

MARCEL DEKKER, INC.
270 Madison Avenue, New York, New York 10016

Table 1. Modification of PIRA Gel Chemical Composition

Compound	Range of Concentration Changes
Bovine serum albumin	5%, 6%, 7%, 8% by weight
Acrylamide co-monomers	6%, 8%, 10%, 12% by weight
N,N′-methylene-bis-acrylamide	50% C
$Fe(NH_4)_2(SO_4)_2 \times 6H_2O$	0.25 mM, 0.5 mM, 1 mM, 2.5 mM Fe^{2+}
$Fe(NH_4)(SO_4)_2 \times 12H_2O$	0.25 mM, 0.5 mM, 1 mM, 2.5 mM Fe^{3+}
H_2SO_4	50 mM, 100 mM

%C is the bis weight fraction per total amount of the co-monomer.

Irradiation of the Samples

The irradiation was performed using a γ Co-60 beam from ALCYON II (GE-CGR MeV, Buc, France) and T-780 (Theratronics, Canada) therapy units. For the NMR or spectrophotometric dose-response experiments, the gels and Fricke solutions samples were irradiated in NMR test tubes or UV grade acrylic cuvettes, respectively, embedded in specially built polystyrene phantoms. The samples containing the dosimetric material were irradiated with a large field size, at a depth of dose maximum (5 mm tissue equivalent) in a polystyrene block to provide full scatter and build-up conditions. The dose rate was about 200 cGy/min. The doses ranged from 0 to 45 Gy and were confirmed by irradiating calibrated $Li_2B_4O_7$ thermoluminescent powder under the same conditions.

Measurement of the Relaxation Times

The measurements of the longitudinal proton relaxation time T1 were performed in a 0.48 T, 20 MHz for proton, spectrometer (Bruker, PC 20, Wissenburg, France). T1 was measured by inversion recovery, using eight values for the pulse delays and a three-parameter nonlinear least squares fit to the data. The gels were measured directly before and after irradiation in the same tubes. All measurements were carried out at 21 °C ± °C and about two hours after the production of the gel samples.

Absorption, Emission, and Emission Anisotropy Measurements

The gels and Fricke solution samples were measured in the UV-grade acrylic 1cm square cross-section cuvettes (SARSTEDT 100 No.67755), the same one in which they were irradiated earlier. All measurements were carried out at 21 °C ± 1 °C.

Marcel Dekker, Inc.
270 Madison Avenue, New York, New York 10016

Absorbance was measured on a Specord M40 (Carl Zeiss, Jena, Germany) spectrophotometer at a wavelength of 304 nm, i.e. at the maximum of the Fe^{3+} absorption spectrum.

Fluorescence spectra were recorded upon front face excitation using the fully corrected spectrophotometer described previously[34]. Gel samples were excited at 340 nm. Fluorescence spectra were scanned from 350 to 500 nm.

Fluorescence anisotropy was measured by the photon counting technique as described previously[35]. The excitation and observation wavelengths were 340 and 400 nm, respectively.

RESULTS

Figure 1 shows the effect of the concentration of Fe^{2+} ions in the PIRA gel on the $R1$ values in the 0–30 Gy dose range. An increase in the initial Fe^{2+} ion concentration resulted in an increase in the initial $R1$, and also in the d values – the slope of the $R1$ dose-response curves. $R1$ changed according to the absorbed dose, mainly due to the well-established effect of the oxidation of ferrous to ferric ions upon irradiation in the presence of organic substances and oxygen. The NMR observations were confirmed by spectrophotometric measurements. Figure 2 presents the absorbance changes of the PIRA gel after the irradiation with different doses at a wavelength of 304 nm. The investigated substance had initial concentrations of 0.5 mM Fe^{2+} ions and 100 mM H_2SO_4. The dashed line represents the fitted curve by the least square method for the PIRA. The absorbance values increased with the absorbed dose as the concentration of ferric ions increased. The $R1$-dose dependence of the ferrous sulphate doped-protein dosimeter is shown in Fig. 3 for PIRA gels containing 5% and 8% of bovine serum albumin at two sulphuric acid concentration values. The results indicate that the NMR dose sensitivity decreases with increasing BSA concentration and increases with increasing H_2SO_4 concentration. To study the structural changes of BSA molecules generated by irradiation, pyrene was used as a fluorescent probe. Figure 4 presents fluorescence spectra of the PIRA gel doped with pyrene. Emission bands of all the samples did not differ markedly, and the ratio of the third peak to the first peak (III/I) remained constant in the dose interval investigated (0–45 Gy). Figure 5 shows relative changes in longitudinal relaxation rates $R1$ for PIRA gel with different total amount of polymer co-monomers, but with equal fraction of the crosslinker bis (50%C), as a function of the absorbed dose. The data plotted show that the dose-responses were similar, despite augmentation of polymer concentration from 6% to 12%. The emission anisotropy measurements of the PIRA gel

MARCEL DEKKER, INC.
270 Madison Avenue, New York, New York 10016

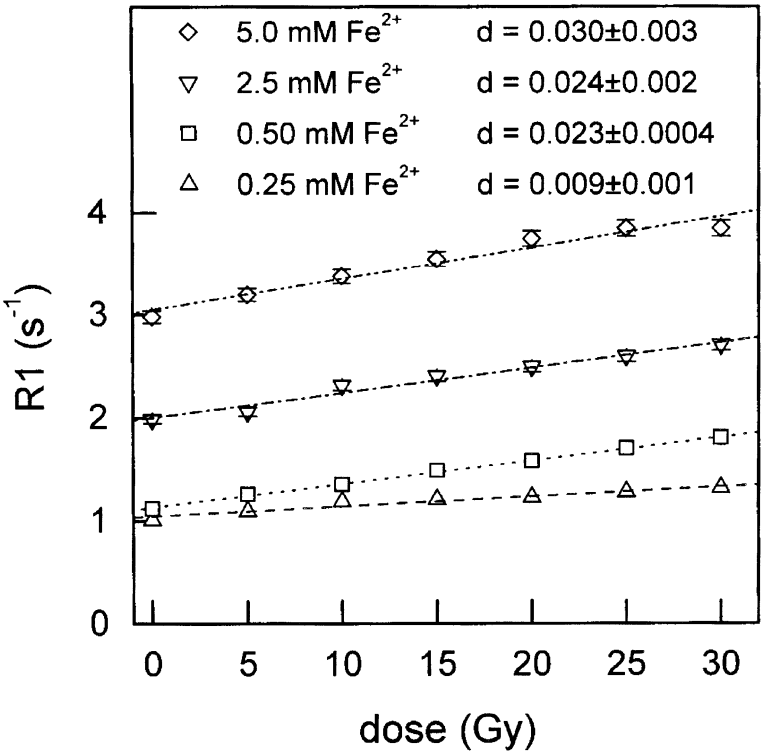

Figure 1. Initial ferrous ion concentration dependence of the dose-response curves R1 of the PIRA gel containing 5% BSA, 10% acrylamide with 50% C bis. The measurement errors are smaller than the data symbols for 0.25 and 0.5 mM Fe^{2+} ion concentrations.

samples also indicate the negligible influence of the irradiation on the gel structure (Fig. 6). The values of the anisotropy, r, were about 0.2 for all samples irradiated with different doses.

DISCUSSION AND CONCLUSIONS

The aim of measurements NMR and optical spectroscopy, was to determine the mechanism responsible for the increase in $R1$ with the dose absorbed. The dose dependence of $R1$ in the PIRA gel was reproducible and was linear up to about 30 Gy, with a slope of $0.023\,s^{-1}Gy^{-1} \pm 2\%$ at 0.48 T[32]. The dependence of the dose-response curves on the Fe^{2+}

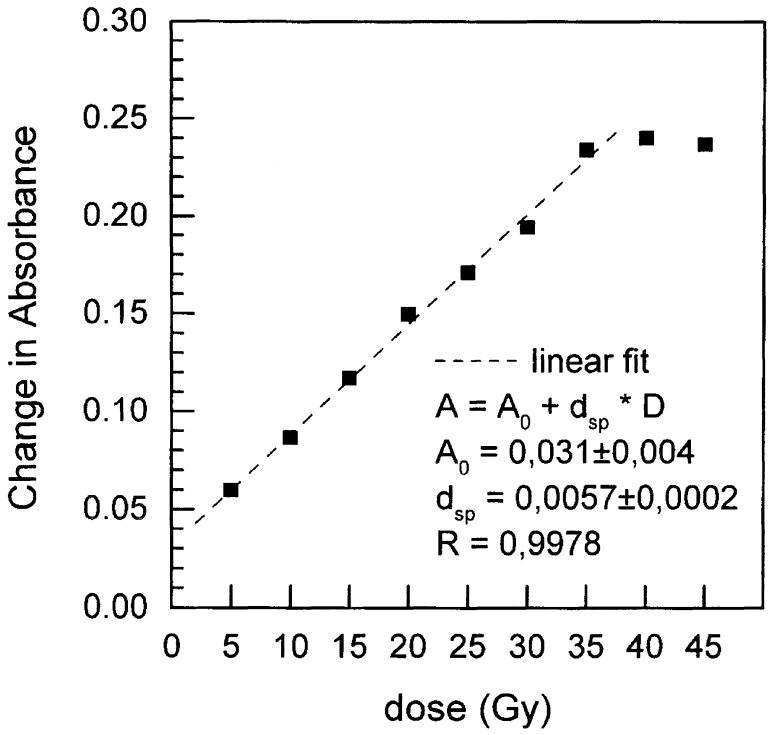

Figure 2. Spectrophotometric absorbance-dose response for the PIRA gel containing 0.5 mM Fe^{2+} and 100 mM H_2SO_4.

concentration (Fig. 1), suggested that the mechanism investigated is the same as in other Fricke-doped dosimetric gels. Similarly as for gels containing gelatin[16] or agarose[15] the initial value of $R1$ increases with the increasing Fe^{2+} concentration, as well as the slope of the dose response-curves for concentrations up to about 0.5 mM. Nonetheless, radiosensitivity of the PIRA gel was lower than that of gels studied earlier with equal Fe^{2+} ion concentration.

Spectrophotometric measurements were carried out to validate the NMR observations (Fig. 2). The observation of the ferric ions absorption peaks could be accomplished only at 304 nm because of the strong absorption by protein at 224 nm. The spectrophotometric dose sensitivities, given in Gy^{-1}, determined as the slope of the line fitted to experimental points of the absorbance versus the dose plot, were 0.0055 for PIRA gel and 0.0068 for Fricke solution with the same initial Fe^{2+} ions and H_2SO_4 concentrations. The PIRA gel dose sensitivity value was lower than those

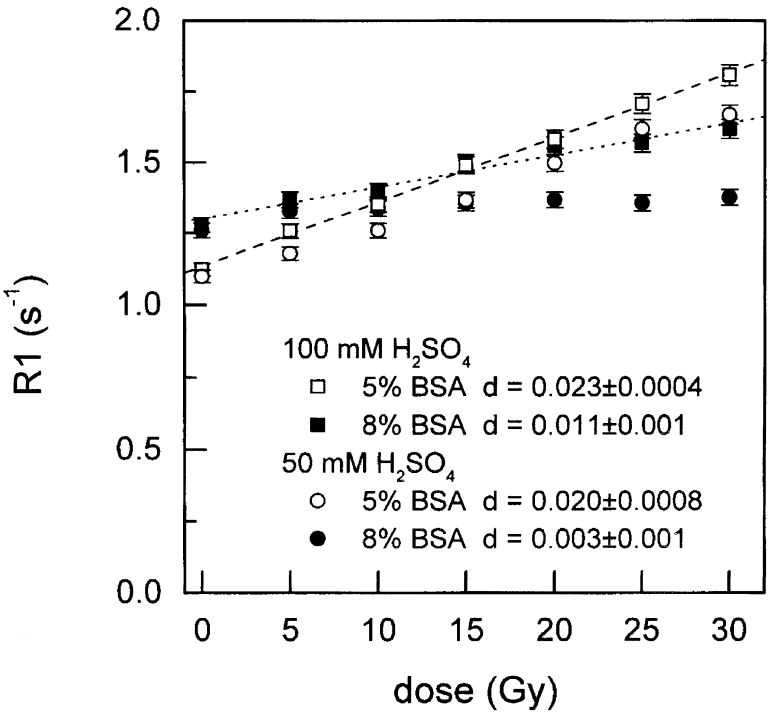

Figure 3. BSA and sulphuric acid concentration dependence of the dose-response curves R1 of the PIRA gel containing 10% acrylamide with 50% C bis and 0.5 mM Fe^{2+}. The dashed line represents the linear fit to the R1 response for 5% BSA and the dotted line for 8% BSA with the same (100 mM) sulphuric acid concentration.

reported by Audet and Schreiner[30] for the Fricke-gelatin dosimeters, but it should be noted that their initial Fe^{2+} concentration was twofold higher than that recorded in the PIRA gel.

The influence of various concentrations of BSA and polyacrylamide on the NMR dose sensitivity was studied by $R1$ measurements as a function of the dose. Initial concentrations of the Fe^{2+} ions were held constant. The increase in the BSA concentration and pH in the PIRA gel reduced the slope of the dose-response curve (Fig. 3). This is consistent with results obtained for doped-gelatin dosimeter gels[30]. Protein, similarly to gelatin[28], may affect radiosensitivity indirectly, by affecting the initial pH of the dosimetric substance, or directly by binding with the ion during the preparation process. The amphoteric properties of BSA can increase the pH and, consequently, lower the radiosensitivity. The influence of pH on the dose

MARCEL DEKKER, INC.
270 Madison Avenue, New York, New York 10016

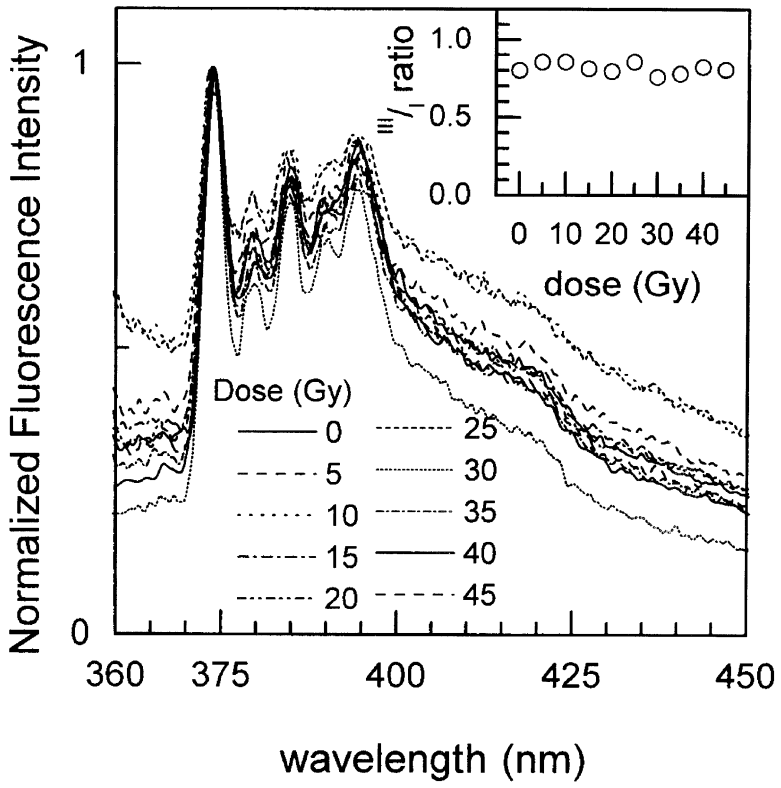

Figure 4. Fluorescence spectra of the irradiated PIRA gel doped with pyrene.

sensitivity of other Fricke doped gels were reported earlier and showed that an increase in pH, by lowering the H_2SO_4 initial concentration, results in a lower dose sensitivity[7,15,28]. The possible radiation-induced changes in BSA were studied by fluorescence measurements of pyrene attached to the PIRA gel. This molecule is widely applied as a fluorescent probe in investigations of various properties of hydrogels, polymers, proteins and membranes since its fluorescence is highly dependent upon local environment[33,36,37]. The vibrational structure of pyrene fluorescence spectra transforms when the polarity of the environment changes. This structure is frequently characterized by the ratio of the third peak to the first peak, which is commonly referred to as the III/I ratio. As the solvent or medium becomes more hydrophobic, the III/I ratio increases. Pyrene is insoluble in water, but it was solubilized by BSA in an aqueous solution, since it embeds in the BSA molecules. When the BSA undergoes structural changes as a result of irradiation, the pyrene

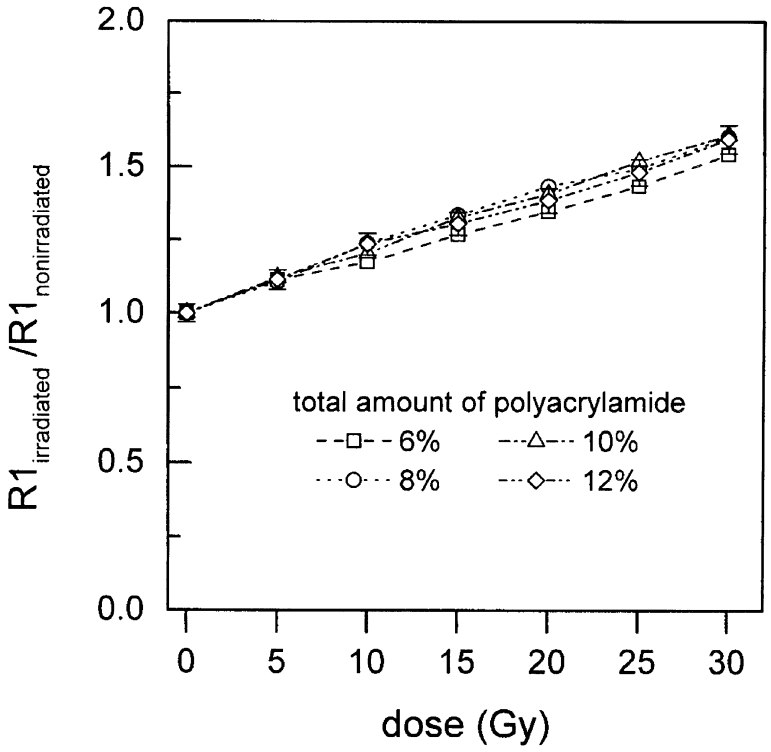

Figure 5. Dependence of the dose response curves of the PIRA gel containing 5% BSA, 0.5 mM Fe^{2+}, and 100 mM H_2SO_4 on the total amount of polyacrylamide with 50% C crosslinker bis. Some measurement errors are shown.

molecules can be ejected to the aqueous phase, which should be associated with the decrease in both the III/I ratio and fluorescence intensity. Fluorescence spectra of pyrene molecules doped to the PIRA gel were measured prior to and after irradiation with different doses. The III/I ratio obtained did not change after the irradiation (Fig. 4). This is an expected result because the aggregation and radiation-induced fragmentation of BSA in the presence of oxygen require higher doses, on the level of hundreds of Gray[38,39].

The dose-response *R*1 of the PIRA gel did not change with the variation of the total amount of acrylamide co-monomers (Fig. 5). This seems rational since the presence of oxygen inhibits the radiation-induced processes occurring in polymer dosimetric gels[40]. The primary mechanism of the response of the polymer gels to radiation is a free radical chain poly-

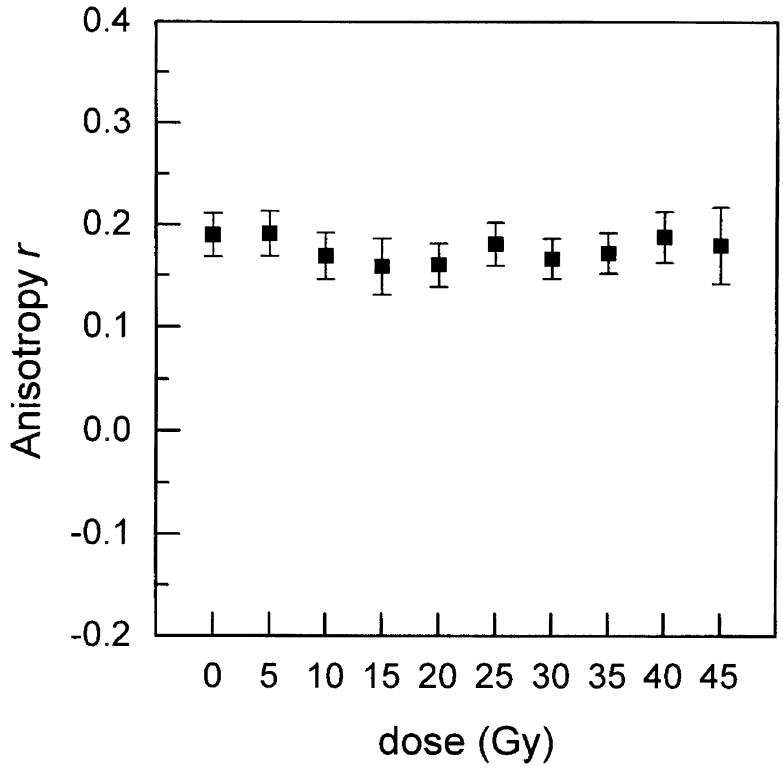

Figure 6. The emission anisotropy, r, of the irradiated PIRA gel as a function of the absorbed dose.

merization initiated by free radical products of water radiolysis[5]. The radiation induced and dose dependent changes can be investigated by NMR study: relaxation times measurements[29,41] magnetization transfer measurements[42,43] and by spectrophotometric study[44,45]. Changes in the structure of the gel, influencing its rigidity and local viscosity can be investigated by means of emission anisotropy measurements. The emission anisotropy is defined by

$$r = \frac{I_{\parallel} - I_{\perp}}{I} \tag{1}$$

where $I = I_{\parallel} + 2I_{\perp}$ is the total fluorescence intensity, and $I_{\parallel}$ and $I_{\perp}$ are components parallel and perpendicular to the direction of the electric vector

of the exciting light, respectively. The maximum value of the fluorescence emission anisotropy (the so-called fundamental anisotropy) for isotropic solution equals 0.4. The fact that the measured values of the anisotropy, r, for the PIRA gel are markedly lower (Fig. 6) indicates that irrespective of the rigidity of the medium, restricted rotational motions may occur. The behaviour of the anisotropy values is governed by the Perrin equation[46]:

$$\frac{r_0}{r} = 1 + \chi \tag{2}$$

In this equation, describing rotational depolarization of fluorescence, an important role is played by the dimensionless constant

$$\chi = \frac{kT}{V} * \nu = \frac{\tau}{\tau_D} \tag{3}$$

where τ is the fluorescence lifetime, τ_D is the rotational relaxation time, V is the volume of the luminescent molecule embracing the solvent shell, ν is the dynamic viscosity of the solvent, and r_0 is the fundamental emission anisotropy. Since under the experimental conditions the fluorescence lifetime of pyrene molecules remains constant, so do the anisotropy values measured. Thus, the rotational relaxation time also remains constant. This data indicates that the dynamic viscosity of the local environment of pyrene molecules is not affected by irradiation.

The fluorescence spectroscopy measurements of the PIRA gel demonstrated that the main mechanism responsible for the increase in the relaxation rate, $R1$, proportional to the absorbed dose, is the radiation-induced oxidation of ferrous to ferric ions. Also, there is no influence on $R1$ as a result of structural changes in the protein-polymer matrix. This fact allows us to apply the four-site fast exchange model proposed by[30] for the $R1$-dose response of the ferrous sulphate doped-gelatin dosimeter. This model assumes that the spin-lattice relaxation is determined principally by protons on water molecules in the system. These protons exist in four different types of environment (bulk water, water hydrating the Fe^{2+} and Fe^{3+} ions, and water hydrating gel matrix). Water is expected to exchange quickly between the four environments, so the relaxation rate is simply the sum of the inherent rates $R1^i$, each weighted by the fraction of protons, p^i, in their respective groups:

$$R1 = \sum_{i=4} p^i R1^i \tag{4}$$

MARCEL DEKKER, INC.
270 Madison Avenue, New York, New York 10016

Assuming that initially the Fe^{3+} concentration in the dosimetric gel equals 0 and the radiation-induced changes in the Fe^{3+} concentration in mM are proportional to the absorbed dose D, Audet and Schreiner obtained:

$$R1 = \left\{ G(Fe^{3+})(r^{3+} - r^{2+}) \frac{10\rho}{N_{A^e}} \right\} D + R_0 = dD + R_0 \tag{5}$$

where $G(Fe^{3+})$ is the number of Fe^{3+} ions produced per 100 eV, r^{3+} and r^{2+} are relaxivities of the respective solutes, ρ is the density in kg/l, N_A is the Avogadro number, e is the number of Joules/eV, R_0 is a constant for a given gelatin concentration, and the coefficient d is the dose sensitivity of the dosimeter.

The G values determined independently using the NMR technique and spectrophotometry provide a tool for verifying the model described above[30]. The NMR G value can be determined from the NMR dose sensitivity and the Fe^{2+} and Fe^{3+} relaxivity data:

$$G(Fe^{3+}) = d \frac{1}{r^{3+}_{reff} - r^{2+}} \frac{N_A e}{10\rho} \tag{6}$$

r^{3+}_{reff} is the effective relaxivity of the Fe^{3+} ion complexes in a particular gel dosimeter.

The spectrophotometric G value can be determined from the extinction coefficient, ε, and the spectrophotometric dose sensitivity d_{sp}:

$$G(Fe^{3+}) = d_{sp} \frac{1}{\varepsilon} \frac{N_A e}{10\rho} \tag{7}$$

ε, the extinction coefficient characterizes the change in absorbance per unit optical path length as the Fe^{3+} ion concentration is changed. The G values calculated for the PIRA gel and corresponding the NMR and spectrophotometry data are presented in Table 2. The density of the PIRA gel was taken as $\rho = 1.03\,kg/l$[32].

The calculated NMR G value agrees with the spectrophotometric G value within the experimental error, but is higher than the ferric ion chemical yield of 15,6 Fe^{3+} ions/100 eV for aqueous Fricke solution containing 0.4 mM H_2SO_4[47]. This is likely to result from the presence of the BSA, which, like an organic additive, sensitises the standard dosimeter[48]. None the less, this G value is lower than the values reported for the Fricke doped gel dosimeters including gelatin[28,30] and agarose[15,48]. Compared with gelatin-based dosimeters, the PIRA gel shows lower $R1$-dose sensitivity but the same ferrous ion relaxivity and very similar (within the experimental error)

MARCEL DEKKER, INC.
270 Madison Avenue, New York, New York 10016

Table 2. The NMR and Spectrophotometric G Values for the PIRA Gel

NMR				Spectrophotometry		
r_{eff}^{3+} ($s^{-1}\,mM^{-1}$)	r^{2+} ($s^{-1}\,mM^{-1}$)	d ($s^{-1}\,Gy^{-1}$)	G $Fe^{3+}/100\,eV$	ε ($mM^{-1}\,cm^{-1}$)	dsp (Gy^{-1})	G $Fe^{3+}/100\,eV$
8.65 ± 0.37	0.42 ± 0.01	0.023 ± 0.0005	26.1 ± 1.3	1.9499 ± 0.017	0.0055 ± 0.0004	26.4 ± 1.9

MARCEL DEKKER, INC.
270 Madison Avenue, New York, New York 10016

the ferric ion relaxivity. The $R1$ dose sensitivity of the PIRA gel, as well as gelatin-based dosimeters depends on the pH and increases with the increasing sulphuric acid concentration. The improvement in the $R1$ dose-response by augmentation of the acid content is limited due to the degradation of mechanical properties of the gel. The behaviour of the Fricke-doped protein-polymer system at different acid concentrations and its influence for dose sensitivity requires further investigation.

The NMR and optical spectroscopy studies allow us to determine the main mechanism responsible for the $R1$ dose dependence of the PIRA gel and, consequently, to apply the four-site effective fast exchange model proposed by Audet and Schreiner[30] for obtaining the ferric ions chemical yield value. The agreement between the values of $G(Fe^{3+})$ calculated from the NMR data and, independently, from spectrophotometrical measurements proved that absolute dosimetry in the case of Fricke-doped NMR phantom substances is possible. Less promising results concern the NMR dosimetry of real biological systems[49], with a still lacking model describing the radio-induced changes in the relaxation times.

ACKNOWLEDGMENTS

The authors would like to thank the Department of Radiotherapy in the Centre Eugene Marquis in Rennes and the Department of Oncology and Radiotherapy of the Medical University of Gdansk for allowing the use of their irradiation units. The help of Dr. François Husson, Mrs Renata Nowak and Mr Piotr Szewczyk in sample irradiation is appreciated. The authors are particularly grateful to Dr. Grzegorz Piszczek, Department of Biochemistry, University of Maryland for many useful tips and discussions regarding optical spectroscopy experiments. This work was supported by KBN (Committee on Scientific Research) grant No. 2PO3B 148 12 (Poland). G.Z. was supported by 93/2155 grant from CNOUS, Paris.

REFERENCES

1. Gore, J.C.; Kang, Y.S.; Schulz, R.J. Measurement of Radiation Dose Distributions by Nuclear Magnetic Resonance (NMR) Imaging. Phys. Med. Biol. **1984**, *29*, 1189–1197.
2. Gore, J.C.; Kang, Y.S.; Schulz, R.J. The Measurement of Radiation Dose Distributions by Magnetic Resonance Imaging. Magn. Reson. Imaging **1984**, *2*, 244.

3. Appleby, A.; Christman, E.A.; Leghrouz, A. Imaging of Spatial Dose Distribution in Agarose Gels Using Magnetic Resonance. Med. Phys. **1987**, *14*, 382–384.
4. Olsson, L.E.; Petersson, S.; Ahlgren, L.; Mattsson, G. Ferrous Sulphate Gels for Determination of Absorbed Dose Distributions Using MRI Technique: Basic Studies. Phys. Med. Biol. **1989**, *34*, 43–52.
5. Maryanski, M.J.; Gore, J.C.; Kennan, R.P.; Schulz, R.J. NMR Relaxation Enhancement in Gels Polymerized and Cross-Linked by Ionizing Radiation: A New Approach to 3D Dosimetry by MRI. Magn. Reson. Imaging **1993**, *11*, 253–258.
6. Maryanski, M.J.; Ibbott, G.S.; Schulz, R.J.; Gore, J.C. Radiation Therapy Dosimetry Using Magnetic Resonance Imaging of Polymer Gels. Med. Phys. **1996**, *23*, 699–705.
7. Olsson, L.E.; Fransson, A.; Ericsson, A.; Mattsson, G. MR Imaging of Absorbed Dose Distributions for Radiotherapy Using Ferrous Sulphate Gels. Phys. Med. Biol. **1990**, *35*, 1623–1631.
8. de Guzman, A.F.; Gore, J.C.; Schulz, R.J. Dose Response Curves for Gels Infused with Fricke Dosimeter by NMR. Med. Phys. **1989**, *16*, 457.
9. Hiraoka, T.; Fukuda, N.; Ikehira, H.; Hoshino, K.; Tateno, Y.; Kawashima, K. Digital Imaging of Dose Distributions using NMR Imager. Nipp. Acta Radiol. **1992**, *52*, 1177–1182.
10. Hiraoka, T.; Hoshino, K.; Kawashima, K.; Hirotoshi, K.; Tateno, Y. A New Gel Using Super Absorbent Polymer for Mapping the Spatial Dose Distributions of Electron Beams by MR Imager. Med. Dosim. **1993**, *18*, 73–79.
11. Rouselle, I.; Castelain, B.; Coche-Dequeant, B.; Sarrazin, T.; Rousseau, J. Contrôle de Qualité Dosimétrique en Radiothérapie Stéréotaxique à L'aide de Gels Radiosensibles. Cancer/Radiother **1998**, *2*, 139–145.
12. Zebrowska, G.; Husson, F.; Lewa, Cz. J.; de Certaines, J.D. MRI of Radiation Dose Distributions in a New Tissue Equivalent Gel Dosimeter (PIRA) *SRMBM Book of Abstracts*, *Nice 1995*, 1995, p. 1102.
13. Kron, T.; Metcalfe, P.; Pope, J.M. Investigation of the Tissue Equivalence of Gels Used for NMR Dosimetry. Phys. Med. Biol. **1993**, *38*, 139–150.
14. Chan, M.F.; Ayyangar, K. Verification of Water Equivalence of FeMRI Gels Using Monte Carlo Simulation. Med. Phys. **1995**, *22*, 475–478.
15. Schulz, R.J.; de Guzman, A.F.; Nguyen, D.B.; Gore, J.C. Dose-Response Curves for Fricke-Infused Agarose Gels as Obtained

MARCEL DEKKER, INC.
270 Madison Avenue, New York, New York 10016

by Nuclear Magnetic Resonance. Phys. Med. Biol. **1990**, *35*, 1611–1622.
16. Hazle, J.D.; Hefner, L.; Nyerick, C.E.; Wilson, L.; Boyer, A.L. Dose-Response Characteristics of a Ferrous-sulphate Doped Gelatin Systems for Determining Radiation Absorbed Dose Distributions by Nuclear Magnetic Resonance (Fe MRI). Phys. Med. Biol. **1991**, *36*, 1117–1125.
17. Oldham, M.; McJury, M.; Baustert, I.B.; Webb, S.; Leach, M.O. Improving Calibration Accuracy in Gel Dosimetry. Phys. Med. Biol. **1998**, *43*, 2709–2720.
18. Ibbott, G.S.; Maryanski, M.J.; Eastman, P.; Holcomb, S.D.; Zhang, Y.; Avison, R.G.; Sanders, M.; Gore, J.C. Three-Dimensional Visualization and Measurement of Conformal Dose Distributions Using Magnetic Resonance Imaging of BANG Polymer Gel Dosimeters. Int. J. Radiat. Oncol. Biol. Phys. **1997**, *38*, 1097–2103.
19. Knutsen, B.H.; Skretting, A.; Hellebust, T.P.; Olsen, D.R. Determination of 3D Dose Distribution from Intracavitary Brachytherapy of Cervical Cancer by MRI of Irradiated Ferrous Sulphate Gel. Radiother. Oncol. **1997**, *43*, 219–227.
20. Johansson, S.A.; Magnusson, P.; Fransson, A.; Olsson, L.E.; Christoffersson, J-O.; Montelius, A.; Mattsson, S. Dosimeter Gel and MR Imaging for Verification of Calculated Dose Distributions in Clinical Radiation Therapy. Acta Oncol. **1997**, *36*, 283–290.
21. Oldham, M.; Baustert, I.; Lord, C.; Smith, T.A.; McJury, M.; Warrington, A.P.; Leach, M.O.; Webb, S. An Investigation into the Dosimetry of a Nine-Field Tomotherapy Irradiation Using BANG-Gel Dosimetry. Phys. Med. Biol. **1998**, *43*, 1113–1132.
22. Rouselle, I.; Castelain, B.; Coche-Dequeant, B.; Sarrazin, T.; Rousseau, J. Contrôle de Qualité Dosimétrique en Radiothérapie Stéréotaxique à L'aide de Gels Radiosensibles. Cancer/Radiother **1998**, *2*, 139–145.
23. Gambarini, G.; Arrigoni, S.; Cantone, M.C.; Molho, N.; Facchielli, L.; Sichirollo, A.E. Dose-Response Curve Slope Improvement and Result Reproducibility of Ferrous-Sulphate-Doped Gels Analyzed by NMR Imaging. Phys. Med. Biol. **1994**, *39*, 703–717.
24. Baldock, C.; Burford, R.P.; Billingham, N.; Wagner, G.S.; Patval, S.; Badawi, R.D.; Keevil, S.F. Experimental Procedure for Manufacture and Calibration of Polyacrylamide Gel (PAG) for Magnetic Resonance Imaging (MRI) Radiation Dosimetry. Phys. Med. Biol. **1998**, *43*, 695–702.
25. Schulz, R.J.; Maryanski, M.J.; Ibbott, G.S.; Bond, J.E. Assessment of the Accuracy of Stereotactic Radiosurgery Using Fricke-Infused Gels and MRI. Med. Phys. **1993**, *20*, 1731–1734.

MARCEL DEKKER, INC.
270 Madison Avenue, New York, New York 10016

26. Kron, T.; Jonas, D.; Pope, J.M. Fast T1 Imaging of Dual Gel Samples for Diffusion Measurements in NMR Dosimetry Gels. Magn. Reson. Imaging **1997**, *15*, 211–221.
27. Johansson, S.A.; Magnusson, P.; Fransson, A.; Olsson, L.E.; Montelius, A.; Holmberg, O.; Andreo, P.; Mattsson, S. Improvements in Absorbed Dose Measurements for External Radiation Therapy Using Ferrous Dosimeter Gel and MR Imaging (FeMRI). Phys. Med. Biol. **1998**, *43*, 261–276.
28. Duzenli, C.; Sloboda, R.; Robinson, D. A Spin-Spin Relaxation Rate Investigation of the Gelatin Ferrous Sulphate NMR Dosimeter. Phys. Med. Biol. **1994**, *39*, 1577–1592.
29. Maryanski, M.J.; Audet, C.; Gore, J.C. Effects of Crosslinking and Temperature on the Dose Response of a BANG Polymer Gel Dosimeter. Phys. Med. Biol. **1997**, *42*, 303–311.
30. Audet, C.; Schreiner, L.J. Multiple-Site Fast Exchange Model for Spin-Lattice Relaxation in the Fricke-Gelatin Dosimeter. Med. Phys. **1997**, *24*, 201–209.
31. Podgorsak, M.B.; Schreiner, L.J. Nuclear Magnetic Relaxation Characterization of Irradiated Fricke Solution. Med. Phys. **1992**, *19*, 87–95.
32. Zebrowska, G.; Husson, F.; Lewa, Cz.; de Certaines, J. Determination of Radiation Dose Distribution by Magnetic Resonance Imaging in the New Tissue Equivalent Gel. Spectroscopy Letters **1997**, *30*, 1249–1261.
33. Rangarajan, B.; Coons, L.S., Scranton, A.B. Characterization of Hydrogels Using Luminescence Spectroscopy. Biomaterials **1996**, *17*, 649–661.
34. Kawski, A.; Piszczek, G.; Kuklinski, B.; Nowosielski, T. Isomerization of Diphenyl Polyenes. Part VIII. Absorption and Fluorescence Properties of 1-Phenyl-4-Diphenylthiophosphinyl Butadiene in Poly(-Vinyl Alcohol) Film. Z. Naturforsch. **1994**, *49a*, 824–828.
35. Kubicki, A. A Universal Photon-Counting Measuring System for Polarized Spectroscopy. Exp. Tech. Phys. **1989**, *37*, 329–333.
36. Glushko, V.; Thaler, M.S.R.; Karp, C.D. Pyrene Fluorescence Fine Structure as a Polarity Probe of Hydrophobic Regions: Behavior in Model Solvents. Arch. Biochem. Biophys. **1981**, *210*, 33–42.
37. Kalyanasundaram, K.; Thomas, J.K. Environmental Effects on Vibronic Band Intensities in Pyrene Monomer Fluorescence and Intensities in Pyrene Monomer Fluorescence and Their Application in Studies of Micellar Systems. J. Am. Chem. Soc. **1977**, *99*, 2039–2044.
38. Schuessler, H.; Davies, J.V. Radiation-Induced Reduction Reactions with Bovine Serum Albumin. Int. J. Radiat. Biol. **1983**, *43*, 291–301.

MARCEL DEKKER, INC.
270 Madison Avenue, New York, New York 10016

39. Schuessler, H.; Schilling, K. Oxygen Effect in the Radiolysis of Proteins. Part 2 Bovine Serum Albumin. Int. J. Radiat. Biol. **1984**, *45*, 267–281.
40. Odian, G. *Principles of Polymerization*; John Wiley & Sons, Inc.: New York, 1991.
41. Maryanski, M.J.; Schulz, R.J.; Ibbott, G.S.; Gatenby, J.C.; Xie, J.; Horton, D.; Gore, J.C. Magnetic Resonance Imaging of Radiation Dose Distributions Using a Polymer-Gel Dosimeter. Phys. Med. Biol. **1994**, *39*, 1437–1455.
42. Kennan, R.P.; Richardson, K.A.; Zhong, J.; Maryanski, M.; Gore, J.C. The Effects of Cross-Link Density and Chemical Exchange on Magnetization Transfer in Polyacrylamide Gels. J. Magn. Reson. B **1996**, *110*, 267–277.
43. Gochberg, D.F.; Kennan, R.P.; Maryanski, M.J.; Gore, J.C. The Role of Specific Side Groups and pH in Magnetization Transfer in Polymers. J. Magn. Reson. **1998**, *131*, 191–198.
44. Gore, J.C.; Ranade, M.; Maryanski, M.J.; Schulz, R.J. Radiation Dose Distributions in Three Dimensions from Tomographic Optical Density Scanning of Polymer Gels: I. Development of an Optical Scanner. Phys. Med. Biol. **1996**, *41*, 2695–2704.
45. Maryanski, M.J.; Zastavker, Y.Z.; Gore, J.C. Radiation Dose Distributions in Three Dimensions from Tomographic Optical Density Scanning of Polymer Gels: II Optical Properties of the BANG Polymer Gel. Phys. Med. Biol. **1996**, *41*, 2705–2717.
46. Perrin, F. La Fluorescence Des Solutions. Induction Moléculaire. Polarisation et Dureé D'émission- Photochimie. Ann. de Physique **1929**, *12*, 169–275.
47. ICRU Radiation Dosimetry: X-rays Generated at Potentials of 5 to 150 kV *ICRU Report 17* (Washington, DC, ICRU) 1970.
48. Appleby, A.; Leghrouz, A.; Christman, E.A. Radiation Chemical and Magnetic Resonance Studies of Aqueous Agarose Gels Containing Ferrous Ions Radiat. Phys. Chem. **1988**, *32*, 241–244.
49. Zebrowska, G. Can Magnetic Resonance Imaging be a Tool for Biodosimetry? *JMRA* in press, 1998.

Received May 12, 1999
Accepted May 25, 2001

MARCEL DEKKER, INC.
270 Madison Avenue, New York, New York 10016

Request Permission or Order Reprints Instantly!